

Discrete Nanoparticle-BSA Conjugates Manipulated by Hydrophobic Interaction

Ruibo Zhong, Yushuang Liu, Ping Zhang, Jingran Liu, Guofen Zhao, and Feng Zhang*

School of Life Science, Inner Mongolia Agricultural University, 306 Zhaowuda Road, Hohhot 010018, China

S Supporting Information



ABSTRACT: Nanoparticle–protein conjugates are promising probes for biological diagnostics as well as versatile building blocks for nanotechnology. Here we demonstrate a facile method to prepare nanoparticles bearing discrete numbers of BSA simply by physical adsorption and electrophoretic isolation, in which the specific amphiphilic properties of BSA play important roles and the number of adsorbed BSA molecules can also be manipulated by tuning the coating extent of nanoparticles by amphiphilic polymer.

KEYWORDS: nanoparticle, BSA, discrete conjugate, physical adsorption, hydrophobic interaction

Nowadays, nanoparticles (NPs) like noble metal NPs, magnetic NPs and quantum dots are widely applied to life sciences as powerful tools for labeling, sensing, imaging, manipulating and even medical treatment, which is mainly due to their unique and excellent physical and chemical properties.¹ It is well-known that NPs synthesized in higher boiling-point solvents possess better qualities in size distribution (monodispersed), superparamagnetism, and fluorescence than those synthesized in aqueous solution, in that the high temperature can reduce the surface defects by the so-called annealing process.² However, higher-boiling-point solvents are normally hydrophobic oils and make the synthesized NPs protected by kinds of hydrophobic surfactants, which cannot be directly used in bioapplications because life enjoys a water environment.³

To transform these NPs from hydrophobic to water-soluble, scientists developed many approaches that can be classified into two kinds of strategies: ligand exchanging⁴ and amphiphilic polymer coating.⁵ Because the ligand exchanging normally requires a higher affinity between the hydrophilic ligand's terminal functional groups and NP's surface atoms than that between the original hydrophobic ligand's functional groups and NP surface atoms, so these kind of approaches are mainly limited by the NP's materials, which eventually depends on whether the ligand with the right chemically matched functional groups are easily obtained.⁶ In addition, ligand exchange usually involves several steps, in which NPs' loss cannot be hundred percent avoided.

Compared with the ligand exchange approach, amphiphilic polymer coating is a more general method that does not

depend on the material properties of NPs, in that the coating principle is based on the hydrophobic interaction between the original protecting hydrophobic ligands and the amphiphilic polymer.⁷ This generality has made the polymer coating approach much more popular than the ligand exchange method, especially when the same surface properties are required for different material NPs in one experiment. More importantly, after polymer coating, the functional groups of the amphiphilic polymer on the NP surface can be used for further covalent coupling with interesting molecules.⁸

With predesigned functional polymer coated NPs, one may think they will smoothly play their roles as expected inside either serum or cells. However, because of the proteins-filled serum and the incredibly crowded cellular environments,⁹ these NPs are inevitably to be surrounded by the biomolecules such as proteins, forming a "corona" as hotly studied recently.¹⁰ The corona formed on the NP surface can completely destroy their predesigned function because the covered proteins alter the chemical properties of NPs. Although scientists have already developed strategies to reduce the nonspecific adsorption of biomolecules to NPs, such as postmodifying PEG or sugar molecules to the polymer-coated NPs,¹¹ hundred percent inhibition never be obtained so far.

Because nature has selected that the adsorption of proteins on NPs is inevitable, why not to make best use of it? As Paul

Received: April 22, 2014

Accepted: November 5, 2014

Published: November 5, 2014

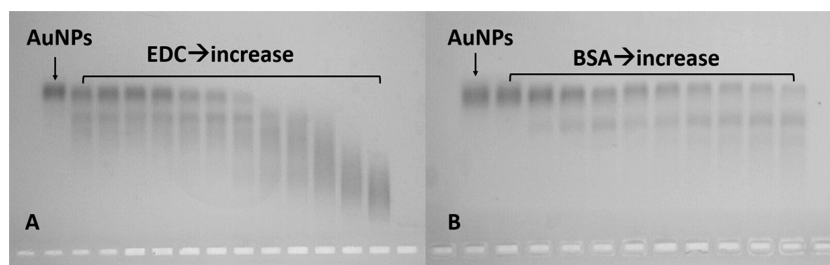


Figure 1. AuNPs with discrete BSA obtained by agarose gel electrophoresis. (A) AuNPs with discrete BSA obtained by EDC coupling. From left to right, the 1st lane is the AuNPs without EDC or BSA as a control, and the rest lanes from left to right are AuNPs mixed BSA with fixed molar ratio (BSA/AuNPs: 500/1) and regularly increased EDC amount, and the molar ratios of EDC to AuNPs are 31.25/1, 62.5/1, 125/1, 250/1, 500/1, 1000/1, 2000/1, 4000/1, 8000/1, 16000/1, 32000/1, and 64000/1, respectively. (B) AuNPs with discrete BSA obtained by physical adsorption. From left to right, the 1st lane is also a control of AuNPs without BSA, and the rest of the lanes are AuNPs mixed with BSA with regularly increased molar ratios (BSA/AuNPs): 50/1, 100/1, 150/1, 200/1, 250/1, 300/1, 350/1, 400/1, 450/1, and 500/1. All the gel electrophoresis was conducted under 4 V/cm, 2% agarose gel was run in TBE ($1 \times$) buffer for 60 min.

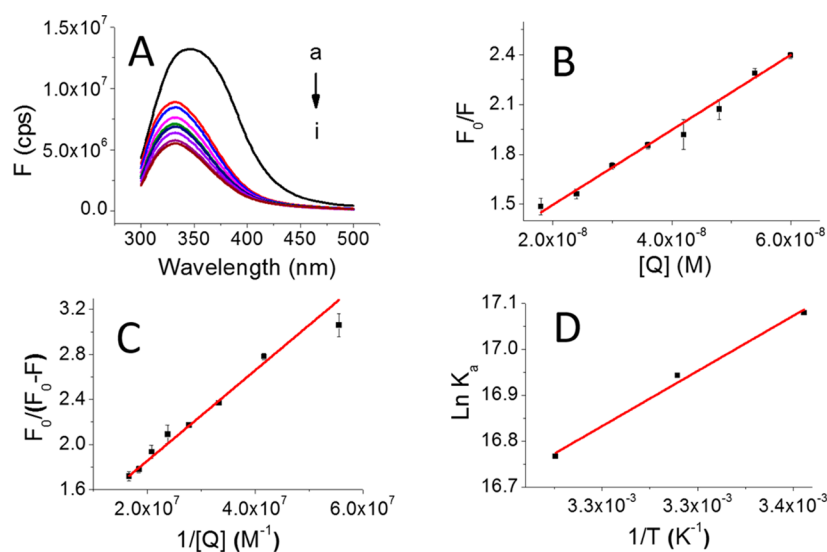


Figure 2. Fluorescence quenching studies on BSA physically adsorbing to AuNPs at 298 K. (A) The corrected steady-state fluorescence spectra of BSA ($0.6 \mu\text{M}$) with various amounts of AuNPs whose concentrations varied (a–i): 0, 18, 24, 30, 36, 42, 48, 54, and $60 \mu\text{M}$, respectively, as represented by an arrow, at 298 K ($\lambda_{\text{ex}} = 280 \text{ nm}$). The fluorescence intensity of the peaks decreased from a to i. (B) Stern–Volmer plot (black dots) and the corresponding linear fit (red line). (C) Modified Stern–Volmer plot (black dots) and the corresponding linear fit (red line). (D) Van't Hoff plot (black dots) at three different temperature (298, 304, and 310 K) and the corresponding linear fit (red line). For all the plots, F and F_0 denote the corrected fluorescence intensities of BSA in the presence and absence of quencher (AuNPs), respectively. And the $[Q]$, K_a , and T represent the concentration of AuNPs, the binding constant of the physical adsorption system, and the absolute temperature, respectively. The error bars were obtained from 3 replicates.

Alivisatos said “because of their unique properties, if NPs could be used as artificial atoms to expand the element table, a number of artificial molecules with the remarkable functions could be obtained by a simply grouping different NPs together via predesigned routes,”¹² which is so-called self-assembly and involves many fields like life sciences and the recently fashionable 4D printer.¹³ Previously, a few literature reported how to obtain the discrete number of biomolecules conjugated with single NP,^{14,15} which is a key issue to further self-assemble NPs to the artificial molecules. Among these papers, single NP with discrete number of ssDNA can be obtained by agarose gel electrophoresis, and later with the complementary properties of base pairs, NPs can be self-assembled into different predesigned patterns,¹⁶ even elegant crystals.¹⁷ More interestingly, with the help of DNA origami, NPs can be grouped into much more complicated predesigned structures,¹⁸ which could be a very promising method so far to fully realize the artificial molecule idea. However, proteins as the other important and potential

molecules in life, are much less studied in the direction to direct NP assembling. Merely one paper we found that reported how to get the single NPs conjugated with discrete number of proteins by a complicated method.¹⁹

Here in this paper, we have developed a facile method to get single NPs conjugated with a discrete number of bovine serum albumin (BSA) just by physical adsorption and electrophoretic isolation, and the amazing affinity between polymer-coated NPs and BSA shows high selectivity among proteins with different kinds of properties and the possible mechanism is discussed.

We took gold NPs (AuNPs, inorganic 5 nm in diameter, and the hydrodynamic diameter is 12 nm) for an example. To get AuNPs with an exact number of BSA molecules, physical adsorption and chemical coupling as a control were studied, respectively. For the chemical coupling, EDC chemistry was employed to form a peptide bond between the carboxylic group of amphiphilic polymer around AuNPs and the amino group on the surface of BSA molecules. From Figure 1A, the bands

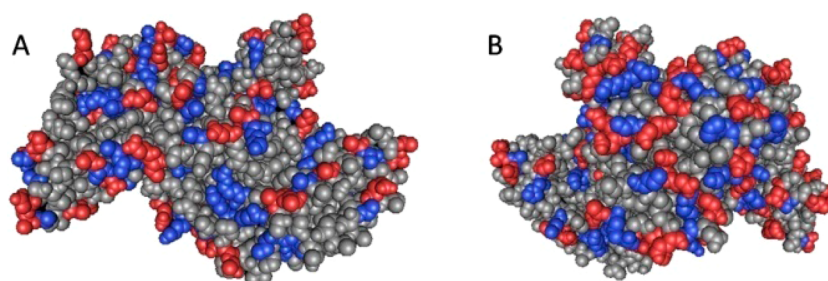


Figure 3. Charge distribution of BSA 3-D molecular structure. The picture is obtained from NCBI database by Cn3D. (A) is the front side of BSA, (B) is the back side of BSA. In this picture, the red color indicates negatively charged residues, the blue color indicates positively charged residues, and the gray color indicates uncharged residues.

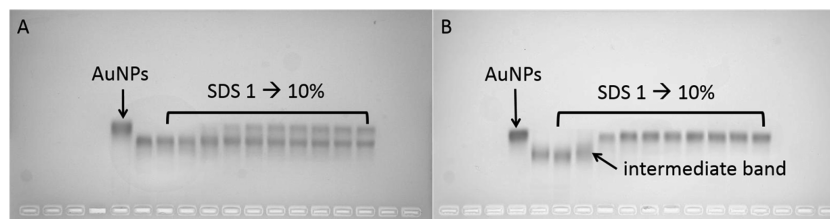


Figure 4. AuNPs with 1 BSA treated by SDS. (A) AuNPs with 1 BSA coupled by EDC chemistry. (B) AuNPs with 1 BSA by physical adsorption. For these 2 gels, from left to right, both the 1st lanes are AuNPs without BSA as controls, and the rest lanes are AuNPs with 1 BSA washed by SDS solution of regularly increased concentrations: 0, 1, 2, 3, 4, 5, 6, 7, 8, 9, and 10%, respectively.

retarded more and more with the EDC increasing (see the Supporting Information, Table S1), indicating more and more BSA molecules were linked to the AuNPs. For the physical adsorption, AuNPs mixed BSA with different molar ratios (see the Supporting Information, Table S2) showed the similar discrete bands on agarose gel (Figure 1B), and there were AuNPs with exact 0, 1 BSA molecules can be clearly separated, indicating there formed a very strong attractive interaction between BSA molecules and AuNPs. The strong affinity was further proved by an additional experiment in which the purified AuNP-BSA complex can resist the second-time gel electrophoresis (see the Supporting Information, Figure S1). Because gel electrophoresis has been believed as a very reliable separation method that normally the weak/nonspecific interactions can be easily broken during the electrophoresis processes. For instance, AuNPs protected by citrate cannot run in agarose gel, because the interaction between citrate and gold cannot resist the strong separation effects caused by both electric fields and the size exclusion, so scientists generally have to make a ligand exchange with phosphines before running these AuNPs in agarose gel.²⁰ However, because the pK_a of carboxylic group is generally less than 5, so both BSA and AuNPs should be negatively charged in basic buffers (such as sodium borate (SB) buffer with a pH of 9.0 and tris borate EDTA (TBE) buffer with a pH of 8.3) which will produce a relatively strong repelling interaction between each other. Then a question naturally comes out: why these two repelling matters can self-assemble together and how the complex can resist the strong electrophoretic isolation.

To this end, fluorescence quenching method (see the Supporting Information) was employed to study both kinetics and thermodynamics of the physical adsorption procedure.²¹ From Figure 2, one can see the fluorescence of BSA was more and more quenched with the increasing addition of AuNPs. The Stern–Volmer quenching constant (which is a measure of the quenching efficiency) was calculated to $2.20 \times 10^7 \text{ M}^{-1}$. Normally, τ_0 of biopolymers is taken as $1 \times 10^{-8} \text{ s}$,²² so the k_q is

determined to $2.20 \times 10^{15} \text{ M}^{-1} \text{ s}^{-1}$. This k_q is much larger than the diffusion-controlled limit (normally near $1 \times 10^{10} \text{ M}^{-1} \text{ s}^{-1}$), which indicated that a static quenching procedure involved in the physical adsorption. Therefore, a modified Stern–Volmer equation (Supporting Information, eq 3) should be used to analyze the quenching data. With the resultant adsorption data at three different temperatures (298, 304, and 310 K) shown in Table S4 in the Supporting Information, it is clear that the K_a is inversely correlated with temperature, which further confirmed that the AuNP-BSA adsorption is initiated by the conjugate formation (static quenching). In addition, the sign and magnitude of the thermodynamic parameters for protein reactions are usually used to identify the kind of main forces contributing to the ligand-protein stability.²³ By using van't Hoff equation (see the Supporting Information, eq 4) and Gibbs–Helmholtz equation (Supporting Information, eq 5), the interaction processes of the current study were found to be spontaneous as evident from negative ΔG^0 values (see the Supporting Information, Table S4). On the other hand, both the negative ΔH^0 (-29.43 kJ/mol/K) and the positive ΔS^0 (45.17 J/mol/K) values indicate that the AuNP-BSA interaction can be spontaneous because the physical adsorption of AuNP-BSA releases heat to environments/surroundings and in fact the ΔS^0 of the whole system including surroundings and AuNP-BSA reaction system should be positive, which is consistent with the second law of thermodynamics.

Some scientists proposed that BSA has positively charged residues (such as lysine, arginine and histidine) on the surface, and which can attract the negatively charged AuNPs, generating the driving force of physical adsorption.²⁴ However, if look at the crystal structure of BSA, one will find that the negatively charged residues (such as glutamine and aspartic acid) and positively charged residues nearly evenly distributed around the surface (Figure 3), and in such basic buffers we believe the negatively charged groups should be completely dissociated, so that the repelling force will be bigger than the attracting force.

Hence, we think the other reason could be the local hydrophobic interaction.

To figure out whether the hydrophobic interaction dominated the adsorption driving force, we employed sodium dodecyl sulfonate (SDS) to cover/reduce those exposed hydrophobic regions (defect sites) on the surface of amphiphilic polymer coated AuNPs. This control experiment was designed by two reasons. First, SDS has a negatively charged hydrophilic “head” which possesses equivalent effects as the carboxylic groups of amphiphilic polymer, so it will still keep the original surface chemical state; Second, SDS is so small that its hydrophobic tails can easily insert into the local hydrophobic sites on both BSA and AuNPs thus can eliminate the driving force. In practice, SDS solutions with different concentrations were added into the both chemically coupled and physically adsorbed complex samples. From Figure 4, we can see that with the increasing of SDS concentration, physically adsorbed BSA molecules completely departed away from the AuNPs. In contrast, chemically coupled BSA molecules only departed nearly 50% away from AuNPs, which indicates the left are covalently coupled, and the intermediate bands in Figure 4B also indicated some of BSA molecules were exchanged by SDS molecules. Some studies claimed that BSA has a free thiol group (-SH) which can form a gold–thiol bond when the BSA adsorbed to the AuNPs,²⁵ however the current control experiments proved that gold–thiol bond was not formed since SDS cannot exchange the gold–thiol bond, this may be due to the amphiphilic polymer contribute a too thick shell (about 3.5 nm determined by dynamic light scattering method, see the Supporting Information, Figure S5A) for BSA to readily touch the real gold material surface.

BSA is believed as an amphiphilic protein, we also took other proteins with different properties (see the Supporting Information, Table S3) to do the adsorption experiments, and the results (see the Supporting Information, Figure S2) showed only human serum albumin (HSA) showed the similar phenomena as BSA did. The reason was believed that HSA has the similar structure and amphiphilic property as BSA's, which indicates the strong affinity caused by physical adsorption has high selectivity of protein structure, and further proves the local hydrophobic interaction is the driving force. Because the PI of protein in a certain buffer can determine the extent of surface charge, and the results showed that neither the more negatively charged proteins (chymotrypsin and pepsin) nor the more positively charged proteins (insulin, hemoglobin, myoglobin, and HRP) showed the similar adsorption phenomena as BSA did, which further proves the local hydrophobic interaction dominates the driving force rather than the electrostatic interaction. In addition, the molecular weight of the protein is also a necessary factor to form the discrete AuNP–protein conjugates. In the Supporting Information, Figure S3, discrete conjugates only formed by bigger proteins such as hemoglobin (64 kDa), HSA (66 kDa), and BSA (66 kDa), but not by the small proteins like insulin (5.8 kDa), chymotrypsin (13 kDa), myoglobin (17 kDa), pepsin (35 kDa), and HRP (34 kDa), which showed the similar molecular weight effect with PEG or DNA experiments reported previously.^{14,15}

The adsorption interaction between proteins and NPs could also influence the EDC coupling efficiency. One can imagine if the repelling force is too big that the particles and proteins will never touch each other, thus how can the coupling reagents such as EDC link them together? To make a test, we took these

eight kinds of proteins to do the EDC coupling with AuNPs. And the results showed BSA still showed the best coupling effect (see the Supporting Information, Figure S3), which indicates the strong affinity between NPs and proteins can highly improve the efficacy of chemical coupling, too.

We have also characterized the conjugates by dynamic light scattering (DLS). The results showed that the AuNP–BSA conjugates are a little bigger than the AuNPs without BSA adsorption in diameter in solution (see the Supporting Information, Figure S5A). There are several papers reported after the adsorption to nanoparticles, the protein's conformation and its secondary structure will be changed.^{10,26} Here in this paper, we have also checked the structural changing by employing circular dichroism (CD). However, the CD results showed that the BSA still kept intact in secondary structure level after adsorbed to AuNPs (see the Supporting Information, Figure S5B). We speculate that the thick polymer shell may act as a “matrix/mattress” to prevent BSA from touching the gold surface, which might be also an advantage for the further nanofabrication to keep the original conformation of the conjugated proteins.

By a simply stoichiometric calculation, we can get the average number of amphiphilic polymer coated on a single AuNPs is 25.²⁷ Because the steric hindrance effect, the amphiphilic polymer has to fold itself to fit for the surface of AuNPs. However, there inevitably exists such a situation: theoretically calculation needs 25.5 polymer to completely cover the surface of AuNPs. In this case, AuNPs surface cannot accommodate such 0.5 polymer. As a compromising result, only 25 polymers can stay on the AuNPs surface, so there are about 20 hydrophobic sites (one amphiphilic polymer has 40 hydrophobic monomer units in average^{27–29}) still exposed on the polymer-coated AuNPs. And because BSA is also an amphiphilic molecule, when they collide with each other, the hydrophobic interaction between their local hydrophobic sites generates a strong affinity. To further prove this hypothesis, we deliberately reduced the amount of amphiphilic polymer during the coating procedure, and got a batch of polymer-coated AuNPs with more defects exposed in solution. Then the physical adsorption experimental results showed AuNPs adsorbed with 2 BSA molecules can be isolated (see the Supporting Information, Figure S4), which further proved the hydrophobic interaction play a significant role for this strong affinity and the discrete number of BSA can be manipulated by tuning the polymer coating extent. We concluded the mechanism to a hypothesis that the main driving force to self-assemble BSA and AuNPs together is the strong hydrophobic interaction between the local hydrophobic parts on their surface, since both BSA and the coating polymer have been considered amphiphilic (Figure 5).

To the best of our knowledge, this could be the first paper to show that the NPs with discrete proteins can be obtained by simply physical adsorption. Compared with the chemical coupling, the physically adsorption shows not only the strong affinity to resist gel electrophoresis, but also shows the easily departing properties by SDS, which might be useful to some specific instances like reversible self-assembly. The reason for the strong affinity proposed in this paper can be also a new mechanism to enrich the NP–Protein interaction theories. From the high selectivity point of view, this strong attraction can be somehow comparable to the “catching bond”³⁰ or the specific interaction between pairs like antibody and antigen, ligand and receptor, aptamer and its substrate, and so on. This specificity

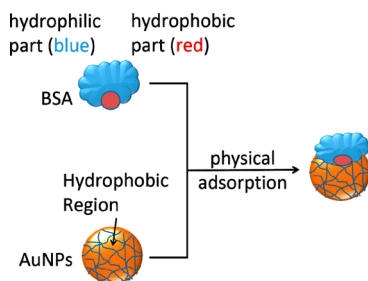


Figure 5. Schematic representation of BSA physically adsorbed to AuNPs. The strong physical adsorption derived from the hydrophobic interaction between BSA (red part) and AuNPs (hydrophobic region).

might need further studying the hydrophobic sequence of BSA/HSA, which may help us to design the *de novo* peptides or fusion proteins for the predesigned nanofabrication. Because the amphiphilic polymer coating does not depend on the NP's material properties, so we believe this facile physical adsorption can be applied to all other polymer coated nanoparticles with different chemical properties as well. Finally, although NP/protein conjugates hold important promises for being the next generation of nanobiosensors or versatile building blocks for nanofabrication, to work in nanoscale biological environments, the amphiphilic polymer coating could never be perfect at avoiding the exposed hydrophobic defects; thus, further techniques still need developing.

■ ASSOCIATED CONTENT

📄 Supporting Information

All the chemicals, instruments and the detailed experimental approaches and calculations. This material is available free of charge via the Internet at <http://pubs.acs.org>.

■ AUTHOR INFORMATION

Corresponding Author

*E-mail: fengzhang1978@hotmail.com.

Notes

The authors declare no competing financial interest.

■ ACKNOWLEDGMENTS

This work was supported by grants from the National Natural Science Foundation of China (21171086, 81160213), and Inner Mongolia Grassland Talent (108-108038), and Inner Mongolia Autonomous Region Natural Science Foundation (2013MS1121) and the Inner Mongolia Agricultural University (211-109003 and 211-206038).

■ REFERENCES

- (1) De, M.; Ghosh, P. S.; Rotello, V. M. Applications of Nanoparticles in Biology. *Adv. Mater.* **2008**, *20*, 4225–4241.
- (2) Garcia-Gutierrez, D. I.; Gutierrez-Wing, C. E.; Giovanetti, L.; Ramallo-Lopez, J. M.; Requejo, F. G.; Jose-Yacaman, M. Temperature Effect on the Synthesis of Au-Pt Bimetallic Nanoparticles. *J. Phys. Chem. B* **2005**, *109*, 3813–3821.
- (3) Brust, M.; Walker, M.; Bethell, D.; Schiffrin, D. J.; Whyman, R. Synthesis of Thiol-Derivatized Gold Nanoparticles in a Two-Phase Liquid-Liquid System. *J. Chem. Soc., Chem. Commun.* **1994**, 801–802.
- (4) Erathodiyil, N.; Ying, J. Y. Functionalization of Inorganic Nanoparticles for Bioimaging Applications. *Acc. Chem. Res.* **2011**, *44*, 925–935.
- (5) Warner, M. G.; Reed, S. M.; Hutchison, J. E. Small, Water-Soluble, Ligand-Stabilized Gold Nanoparticles Synthesized by

Interfacial Ligand Exchange Reactions. *Chem. Mater.* **2000**, *12*, 3316–3320.

(6) Schroedter, A.; Weller, H. Ligand Design and Bioconjugation of Colloidal Gold Nanoparticles. *Angew. Chem., Int. Ed.* **2002**, *41*, 3218–3221.

(7) Pellegrino, T.; Manna, L.; Kudera, S.; Liedl, T.; Koktysh, D.; Rogach, A. L.; Keller, S.; Radler, J.; Natile, G.; Parak, W. J. Hydrophobic Nanocrystals Coated with an Amphiphilic Polymer Shell: A General Route to Water Soluble Nanocrystals. *Nano Lett.* **2004**, *4*, 703–707.

(8) Lin, C. A. J.; Sperling, R. A.; Li, J. K.; Yang, T. Y.; Li, P. Y.; Zanella, M.; Chang, W. H.; Parak, W. G. J. Design of an Amphiphilic Polymer for Nanoparticle Coating and Functionalization. *Small* **2008**, *4*, 334–341.

(9) Nel, A. E.; Madler, L.; Velegol, D.; Xia, T.; Hoek, E. M. V.; Somasundaran, P.; Klaessig, F.; Castranova, V.; Thompson, M. Understanding Biophysicochemical Interactions at the Nano-Bio Interface. *Nat. Mater.* **2009**, *8*, 543–557.

(10) Lynch, I.; Dawson, K. A. Protein-Nanoparticle Interactions. *Nano Today* **2008**, *3*, 40–47.

(11) Zheng, M.; Davidson, F.; Huang, X. Y. Ethylene Glycol Monolayer Protected Nanoparticles for Eliminating Nonspecific Binding with Biological Molecules. *J. Am. Chem. Soc.* **2003**, *125*, 7790–7791.

(12) Choi, C. L.; Alivisatos, A. P. From Artificial Atoms to Nanocrystal Molecules: Preparation and Properties of More Complex Nanostructures. *Annu. Rev. Phys. Chem.* **2010**, *61*, 369–389.

(13) Sharma, K. P.; Collins, A. M.; Perriman, A. W.; Mann, S. Enzymatically Active Self-Standing Protein-Polymer Surfactant Films Prepared by Hierarchical Self-Assembly. *Adv. Mater.* **2013**, *25*, 2005–2010.

(14) Sperling, R. A.; Pellegrino, T.; Li, J. K.; Chang, W. H.; Parak, W. J. Electrophoretic Separation of Nanoparticles with a Discrete Number of Functional Groups. *Adv. Funct. Mater.* **2006**, *16*, 943–948.

(15) Zanchet, D.; Micheel, C. M.; Parak, W. J.; Gerion, D.; Alivisatos, A. P. Electrophoretic Isolation of Discrete Au Nanocrystal/DNA Conjugates. *Nano Lett.* **2000**, *1*, 32–35.

(16) Tan, L. H.; Xing, H.; Chen, H.; Lu, Y. Facile and Efficient Preparation of Anisotropic DNA-Functionalized Gold Nanoparticles and Their Regioselective Assembly. *J. Am. Chem. Soc.* **2013**, *135*, 17675–17678.

(17) Senesi, A. J.; Eichelsdoerfer, D. J.; Macfarlane, R. J.; Jones, M. R.; Auyeung, E.; Lee, B.; Mirkin, C. A. Stepwise Evolution of DNA-Programmable Nanoparticle Superlattices. *Angew. Chem., Int. Ed.* **2013**, *52*, 6624–6628.

(18) Schreiber, R.; Do, J.; Roller, E.-M.; Zhang, T.; Schuller, V. J.; Nickels, P. C.; Feldmann, J.; Liedl, T. Hierarchical Assembly of Metal Nanoparticles, Quantum Dots and Organic Dyes Using DNA Origami Scaffolds. *Nat. Nanotechnol.* **2014**, *9*, 74–78.

(19) Liu, H. Y.; Gao, X. Engineering Monovalent Quantum Dot-Antibody Bioconjugates with a Hybrid Gel System. *Bioconjugate Chem.* **2011**, *22*, 510–517.

(20) Sperling, R. A.; Parak, W. J. Surface Modification, Functionalization and Bioconjugation of Colloidal Inorganic Nanoparticles. *Philos. Trans. R. Soc., A* **2010**, *368*, 1333–1383.

(21) Lakowicz, J. R. *Principles of Fluorescence Spectroscopy*; 3rd ed.; Springer: New York, 2006; p xxvii.

(22) Dewey, T. G. *Biophysical and Biochemical Aspects of Fluorescence Spectroscopy*; Plenum Press: New York, 1991; p xvii, 294 p.

(23) Klotz, I. M. Physicochemical aspects of drug-protein interactions: a general perspective. *Ann. N.Y. Acad. Sci.* **1973**, *226*, 18–35.

(24) Brewer, S. H.; Glomm, W. R.; Johnson, M. C.; Knag, M. K.; Franzen, S. Probing BSA Binding to Citrate-Coated Gold Nanoparticles and Surfaces. *Langmuir* **2005**, *21*, 9303–9307.

(25) Burt, J. L.; Gutierrez-Wing, C.; Miki-Yoshida, M.; Jose-Yacaman, M. Noble-Metal Nanoparticles Directly Conjugated to Globular Proteins. *Langmuir* **2004**, *20*, 11778–11783.

(26) Treuel, L.; Malissek, M.; Gebauer, J. S.; Zellner, R. The Influence of Surface Composition of Nanoparticles on their

Interactions with Serum Albumin. *ChemPhysChem* **2010**, *11*, 3093–3099.

(27) Yakovlev, A. V.; Zhang, F.; Zulqurnain, A.; Azhar-Zahoor, A.; Luccardini, C.; Gaillard, S.; Mallet, J. M.; Tauc, P.; Brochon, J. C.; Parak, W. J.; Feltz, A.; Oheim, M. Wrapping Nanocrystals with an Amphiphilic Polymer Preloaded with Fixed Amounts of Fluorophore Generates FRET-Based Nanoprobes with a Controlled Donor/Acceptor Ratio. *Langmuir* **2009**, *25*, 3232–3239.

(28) Zhang, F.; Lees, E.; Amin, F.; Gil, P. R.; Yang, F.; Mulvaney, P.; Parak, W. J. Polymer-Coated Nanoparticles: A Universal Tool for Biolabelling Experiments. *Small* **2011**, *7*, 3113–3127.

(29) Zhang, F.; Ali, Z.; Amin, F.; Feltz, A.; Oheim, M.; Parak, W. J. Ion and pH Sensing with Colloidal Nanoparticles: Influence of Surface Charge on Sensing and Colloidal Properties. *ChemPhysChem* **2010**, *11*, 730–735.

(30) Forero, M.; Thomas, W. E.; Bland, C.; Nilsson, L. M.; Sokurenko, E. V.; Vogel, V. A Catch-Bond Based Nano adhesive Sensitive to Shear Stress. *Nano Lett.* **2004**, *4*, 1593–1597.